Experimental measurement of shear-induced diffusion in suspensions using long time data

Sameer I. Madanshetty and Ali Nadim
Department of Aerospace and Mechanical Engineering, Boston University, Boston, Massachusetts 02215

H. A. Stone
Division of Applied Sciences, Harvard University, Cambridge, Massachusetts 02138

(Received 19 May 1994; accepted 16 April 1996)

A method based upon Taylor dispersion theory is used to determine the shear-induced diffusion coefficient in concentrated suspensions. The experiments are performed in a cylindrical Couette device with a suspension consisting of polystyrene spheres in a density-matched solution of glycerin and water. A sequence of several hundred transit times for a single tagged sphere to complete successive orbits within the device is measured. The data are analyzed to compute the azimuthal Taylor dispersion coefficient from which the coefficient of shear-induced diffusivity is obtained. In our experiments the particle Reynolds numbers are $\mathcal{O}(10^{-1})$. The experimental results are compared to the existing measurements of the shear-induced diffusion coefficient obtained at lower particle Reynolds numbers and based upon short-time data. We find a shear-enhanced diffusion coefficient $D_\perp/\dot{\gamma}a^2=\mathcal{O}(0.1)$ for a volume fraction of $\phi\approx 0.25$; this is comparable to existing results from previous low particle Reynolds number studies ($\mathcal{R}<10^{-3}$). © *1996 American Institute of Physics.* [S1070-6631(96)01508-5]

I. INTRODUCTION

When a viscous suspension of neutrally buoyant particles is sheared, the particles move on average with the local fluid velocity, but also undergo seemingly random movements, both parallel and perpendicular to the direction of flow, owing to hydrodynamic interactions with the many surrounding particles. Shear-induced diffusion refers to the characterization of these motions via a traditional random walk description. One expects on dimensional grounds that the self-diffusion coefficient D scales as $\dot{\gamma}a^2$ for a particle of radius a experiencing hydrodynamic interactions in a flow with local shear rate $\dot{\gamma}$.

The first measurements of the cross-stream, or lateral shear-induced diffusivity $D_\perp$ as a function of volume fraction ϕ in a sheared suspension with low particle Reynolds numbers ($\mathcal{R}=\dot{\gamma}a^2/\nu<10^{-2}$, where ν is the kinematic viscosity of the suspending fluid) were conducted by Eckstein, Bailey and Shapiro.[1] The experimental procedure was improved by Leighton and Acrivos[2] and recent work by Phan and Leighton[3] has extended the measurements to higher concentrations, $\phi<0.5$ ($\mathcal{R}<2\times10^{-4}$), and to diffusion perpendicular to the plane of the shear. In particular, experimental measurements of successive transit times required for a tagged sphere to complete an orbit in a Couette device are used to calculate the in-plane lateral (i.e., radial) shear-enhanced diffusivity $D_\perp$. Measurements of $D_\perp(\phi)$ have been based upon short-time data because the method of Leighton and Acrivos approximates the Couette flow as a simple shear flow and wall effects are not taken into account. The effect of shear-induced migration on the variation of particle volume fraction in a wide-gap Couette device has been studied using NMR by Abbott *et al.*[4] Brady[5] has used numerical simulations based upon Stokesian dynamics to estimate the shear-induced diffusivity over a wide range of particle Peclet numbers and the limiting result for large Peclet number can be compared to the values reported below.

Recently, Nadim[6] proposed a theoretical scheme based upon Taylor dispersion theory to measure using long-time data the shear-induced self-diffusion coefficient in concentrated suspensions sheared in a Couette device. In this paper, we report experimental measurements of this diffusivity, calculated using the theory of Nadim, for particle-laden suspensions with finite particle Reynolds numbers. Direct comparisons with published results will be made, however, it should be born in mind that our experimental data have particle Reynolds number $\mathcal{O}(10^{-1})$ whereas for the earlier measurements (e.g., Leighton and Acrivos[2]) the corresponding Reynolds numbers were typically $\mathcal{O}(10^{-3})$ or smaller.

II. METHODOLOGY

In this section, we present a brief review of the Taylor dispersion analysis which permits the determination of the shear-induced diffusivity to be made using long-time data of the successive transit times.[6] We also give a procedure for the data analysis that provides an effective means for establishing the correspondence between the experimental results and the theoretical predictions.

A. Background

Consider the transport of a single tagged sphere in a neutrally-buoyant suspension which is sheared in a cylindrical Couette device by rotating one of the cylinders with angular velocity Ω. By using generalized Taylor dispersion theory,[7] Nadim[6] demonstrated that, after a time long enough for the particle to have sampled many times all available radial positions between the cylinders, the transport in the azimuthal direction can be described by the one-dimensional convective-diffusion equation:

$$\frac{\partial P}{\partial t}+\Omega^*\frac{\partial P}{\partial \theta}=D^*\frac{\partial^2 P}{\partial \theta^2}. \tag{1}$$

Here, $P(\theta,t)$ is the probability density for finding the particle in an infinitesimal neighborhood of the azimuthal coordinate θ at time t regardless of the particle's radial position at that time. Also, θ is regarded as ranging from $-\infty$ to ∞ so that its expected value, modulo 2π, is a measure of the number of orbits the particle has completed in the device.

The transport coefficients Ω^* and D^* appearing in (1) are constants which depend on the geometry of the device, the angular velocity of the rotating cylinder and the actual value of the lateral shear-induced diffusion coefficient, the physical parameter which is being sought. Nadim's original analysis assumed that the outer cylinder rotates. Since the experiments reported in this paper are performed in a device in which the inner cylinder rotates with angular velocity Ω, and the outer cylinder is held stationary, here we provide the corresponding expressions for the effective transport coefficients:

$$\frac{\Omega^*}{\Omega}=\frac{R_1^2}{R_2^2-R_1^2}\left[\frac{2R_2^2}{(R_2-a)^2-(R_1+a)^2}\ \ln\left(\frac{R_2-a}{R_1+a}\right)-1\right], \tag{2}$$

$$\frac{D^*}{\Omega}=\frac{AR_1^3R_2^4(R_2-R_1)}{a^2[(R_2-a)^2-(R_1+a)^2](R_2^2-R_1^2)^2\hat{D}_\perp}, \tag{3}$$

where

$$A=H-\frac{3}{2}\alpha H^2+\frac{2}{3}\beta H^3, \tag{4a}$$

$$H=\ln\left(\frac{R_2-a}{R_1+a}\right),\qquad \alpha=\frac{(R_2-a)^2+(R_1+a)^2}{(R_2-a)^2-(R_1+a)^2}, \tag{4b}$$

$$\beta=\frac{(R_2-a)^4+(R_1+a)^4+(R_2-a)^2(R_1+a)^2}{(R_2-a)^4+(R_1+a)^4-2(R_2-a)^2(R_1+a)^2}. \tag{4c}$$

In the above equations, R_1 and R_2 denote, respectively, the radii of the inner and outer cylinders, and a is the radius of the tagged sphere. In addition, $\hat{D}_\perp$ represents the dimensionless lateral shear-induced diffusion coefficient, defined in terms of the dimensional diffusivity, $D_\perp$, and the average fluid shear rate in the Couette gap, $\dot{\gamma}$, by

$$\hat{D}_\perp=\frac{D_\perp}{\dot{\gamma}a^2},\ \text{where}\ \ \dot{\gamma}=\frac{\Omega R_1}{R_2-R_1}. \tag{5}$$

Expression (2) for the mean particle velocity in the azimuthal direction is somewhat different from the case in which the outer cylinder rotates;[6] however, the mean azimuthal dispersivity (3) is exactly the same, which is not surprising since the resulting laminar flow fields created by the rotation of the inner or the outer cylinder differ only by a rigid-body rotation that does not contribute to the Taylor dispersion coefficient. To obtain (3) we have neglected the direct contribution to the effective dispersivity by the azimuthal component of shear-induced diffusivity, $D_\parallel$, since $D_\parallel$ is assumed to be small compared to the terms which have been retained;[6] previous experimental studies have all made this assumption.

The above Taylor dispersion results are based on several assumptions: The velocity profile in the gap between the cylinders is assumed to be identical to that for laminar flow of a viscous Newtonian fluid. The equation describing the detailed transport of a tagged sphere is assumed to be a convective-diffusion equation, with the convective term given in terms of the known laminar velocity profile, and with the diffusive term characterized by a constant (shear-induced) diffusivity, $D_\perp$, in the lateral direction. Since the shear-induced diffusivity is known to be proportional to shear rate $\dot{\gamma}$ and the latter varies across the Couette gap, the use of a constant diffusivity in (1) requires the gap to be narrow so that a nearly uniform shear rate is attained. Furthermore, the particle volume fraction ϕ is assumed to be uniform across the gap. Hydrodynamic interactions of the tagged sphere with the wall are neglected in the derivation, although the excluded volume effect, due to finite particle size, is taken into account so that the center of the tagged sphere is not allowed to approach closer than one particle radius to the wall. With the above assumptions, the particle center samples with equal probability all allowed radial positions r within the gap. Thus, for times longer than the lateral diffusion time, $\mathcal{O}((R_2-R_1)^2/D_\perp)$, the probability for finding the particle center at any radial position between $R_1+a<r<R_2-a$ is constant.

From the cylindrical Couette experiments, the values of the mean angular velocity Ω^* and the mean azimuthal dispersivity D^* can be obtained. Since the geometric parameters of the apparatus and the particle size are known, as is the angular velocity Ω at which the inner cylinder is rotated, comparison of the experimentally determined Ω^* with the predicted value (2) provides a check on the validity of the assumptions incorporated into the theoretical development. The measured values of the mean dispersivity, D^*, are used in conjunction with the theoretical prediction (3) to obtain the dimensionless shear-induced diffusivity, $\hat{D}_\perp$, which appears in the denominator of equation (3).

In our experiments the data collected are the transit times for the tagged sphere to complete successive orbits within the cylindrical Couette device. Typically, several hundred such times are measured during each experimental run. Therefore, it is necessary to devise a scheme to obtain the mean transport coefficients Ω^* and D^* from these measurements. For this purpose, starting with the mean convective diffusion equation (1), which describes the long-time transport, we first derive an expression for the expected probability density of the transit times.

B. Probability density function for the transit times

Consider a particle which is released at $\theta=0$. After some time, by combined mechanisms of diffusion and convection governed by (1), the particle makes one complete orbit, passing $\theta=2\pi$. The probability density for this transit time is obtained by solving (1) subject to the initial condition

$$P(\theta,0)=\delta(\theta), \tag{6}$$

indicating that the particle starts at $\theta=0$. When the particle passes $\theta=2\pi$ (in the direction of increasing θ) the ''first passage'' event has occurred and it is no longer necessary to follow the particle. Therefore, we impose an absorptive boundary condition,

$$P=0, \quad \text{at } \theta=2\pi, \tag{7}$$

which is equivalent to stating that the particle is destroyed as soon as it passes $\theta=2\pi$. Since the range of θ is now restricted to $-\infty<\theta<2\pi$, the total probability at any given time that the particle has passed $\theta=2\pi$ is given by

$$1-\int_{-\infty}^{2\pi} P(\theta,t)\,d\theta. \tag{8}$$

This probability is initially equal to zero [by substitution of (6) into (8)], but increases thereafter toward unity so that after an infinite time, the particle is certain to have passed $\theta=2\pi$. The derivative of (8) with respect to time, therefore, represents the probability density, $f(t)$, that the transit time is between t and $t+dt$:

$$f(t)=-\int_{-\infty}^{2\pi}\frac{\partial P}{\partial t}(\theta,t)\,d\theta. \tag{9}$$

After solving (1) for $\partial P/\partial t$, substituting the result into the integrand of (9), integrating by parts and applying boundary condition (7) and decay conditions at $-\infty$, we arrive at the alternative expression:

$$f(t)=-D^*\left.\frac{\partial P}{\partial\theta}\right|_{\theta=2\pi}. \tag{10}$$

An equation for $f(t)$ is obtained by solving the original convective-diffusion equation using Laplace transformations in time (see the Appendix); this leads to the explicit formula for the probability density function,

$$f(\tau)=\frac{1}{2\sqrt{\pi\tau^3}}\exp\left(q-q^2\tau-\frac{1}{4\tau}\right), \tag{11}$$

where τ is the dimensionless transit time, i.e., the time required for the particle to complete one orbit in the Couette device,

$$\tau=\frac{D^*t}{4\pi^2}, \tag{12}$$

and q is the Peclet number,

$$q=\frac{\pi\Omega^*}{D^*}. \tag{13}$$

The theoretically predicted probability density of transit times, $f(\tau)$, can be compared to a histogram of measured transit times, which serves as a further check for consistency of the original assumptions. Such a comparison of theory and experiment is provided in the discussion of the experimental results.

The mean and variance of τ, based on the probability density (11), are computed explicitly to be

$$\langle\tau\rangle=\frac{1}{2q} \quad \text{and} \quad \langle\tau^2\rangle-\langle\tau\rangle^2=\frac{1}{4q^3}, \tag{14}$$

where $\langle\cdot\rangle$ denotes the usual time average. Converting these results back to dimensional form, we arrive at the final working equations:

$$\frac{\Omega^*}{\Omega}=\frac{2\pi}{\langle\Omega t\rangle}, \tag{15}$$

$$\frac{D^*}{\Omega}=\frac{1}{4\pi}\left(\frac{\Omega^*}{\Omega}\right)^3[\langle\Omega^2t^2\rangle-\langle\Omega t\rangle^2]. \tag{16}$$

From a long sequence of experimentally measured transit times, the mean and the variance are computed. The mean transit time, $\langle t\rangle$, provides the value of the mean angular velocity, Ω^*, of the tagged sphere via (15). Then, the variance of the measured transit times, $\langle t^2\rangle-\langle t\rangle^2$, determines the mean dispersion coefficient, D^*, according to (16). Once these values are known, the dimensionless shear-induced diffusion coefficient can be calculated using (3).

As we shall see later, the data collected in our experiments indicate that the time it takes the particle to complete a *single* orbit in the Couette device is not long enough for Taylor dispersion theory to become applicable. Since from the collected data, it is easy to measure the time it takes for the particle to complete two or more complete orbits in the device, the above analysis is now generalized so as to be applicable to such cases. If the transit time for completing n orbits in the device is denoted by t_n and its dimensionless counterpart is denoted by $\tau_n=D^*t_n/(2n\pi)^2$, the probability density for this multiple-transit time can be shown, using an analysis identical to that in the Appendix, to be

$$f(\tau_n)=\frac{1}{2\sqrt{\pi\tau_n^3}}\exp\left(q_n-q_n^2\tau_n-\frac{1}{4\tau_n}\right), \tag{17}$$

in which $q_n=n\pi\Omega^*/D^*$. Starting with this result, the counterparts of Eqs. (15) and (16), based upon transit times for n complete orbits, are found to be

$$\frac{\Omega^*}{\Omega}=\frac{2n\pi}{\langle\Omega t_n\rangle}, \tag{18}$$

$$\frac{D^*}{\Omega}=\frac{1}{4n\pi}\left(\frac{\Omega^*}{\Omega}\right)^3[\langle\Omega^2t_n^2\rangle-\langle\Omega t_n\rangle^2]. \tag{19}$$

Setting $n=1$ reproduces the previous results.

III. EXPERIMENTAL PROCEDURE

In the Couette flow experiments a single red particle is observed as it moves relative to a density-matched solution containing neutrally-buoyant, identical particles. Transit times for successive complete orbits of the marked particle are measured; the transit times are representative of the average radial location of the particle. The shear-induced diffusivity is calculated from the distribution of transit times as described in Sec. II. In this section we describe the experimental apparatus, particle preparation, the experiments and typical observations.

A. Couette cell

The experiments were performed in a circular Couette apparatus (see Fig. 1). The inner cylinder was rotated while

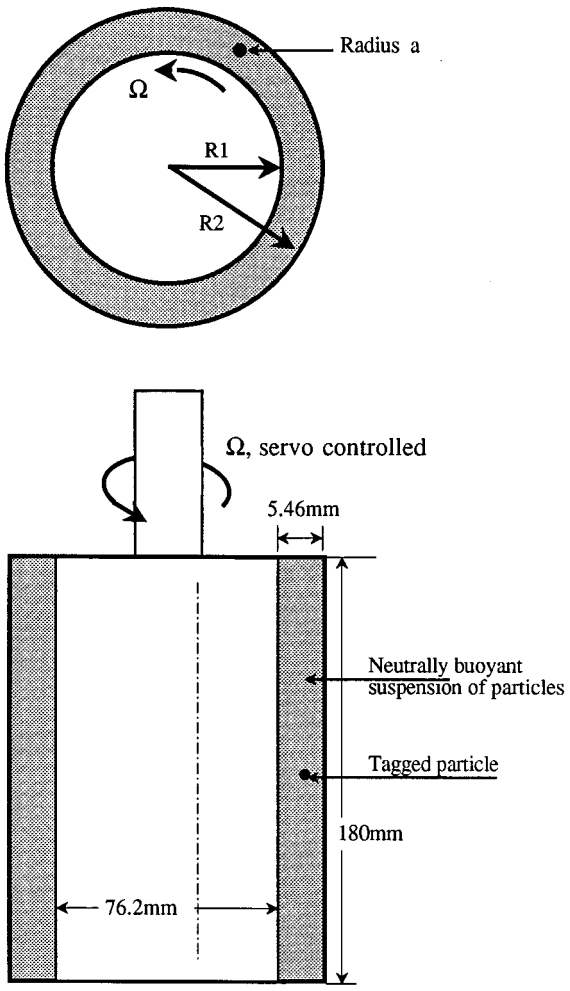

FIG. 1. Schematic of the Couette apparatus.

the outer cylinder remained fixed, and rotation speeds were always lower than the critical rotation rate at which the Taylor-Couette instability began. The white delrin inner cylinder had an outer diameter equal to 6.53 cm$\pm$25 μm and provided a uniform background against which the red colored particle was identified easily. The transparent outer cylinder was made from cast Lucite and had an inner diameter equal to 7.62 cm$\pm$75 μm. The nominal width of the Couette gap was 0.546 cm with an available working height of the annular gap equal to 18 cm. The ratio of the gap width to the inner cylinder radius was 0.167, which is smaller than that used in the Leighton and Acrivos experiments and is less than one-quarter the value reported in the wide-gap experiments of Abbott *et al.*,[4] where volume fraction variations across the gap were measured for cases where the nominal volume fraction was 0.5. The inner cylinder was located in a close-fitting teflon bearing anchored in a base plate, guided at the top in a split bearing, and driven by a vertically mounted reduction drive whose torque and rotation rate were controlled via a servo-controller (ElectroCraft Motomatic-II, Waltham, MA).

A line marked on the stationary outer cylinder served as a reference for the completion of an orbit by the marked particle. Transit times were recorded by an operator striking the return key on the keyboard of a laboratory computer, which utilized an internal reference timing clock to time the transit interval and created a data record of the transit times. We typically used two parallel reference lines marked 90 degrees apart on the outer cylinder. Thus, for each complete orbit of the particle, two measurements for the transit time were obtained. Since the two transit times thus obtained are likely to be correlated, the data were analyzed in several ways, keeping or discarding the data from the second reference line. No effect was found on the final values of the diffusivity. Moreover, since successive transit times obtained from the same reference line are possibly correlated as well, in the analysis we tested the experimental results by discarding up to ten transit time values between the ones that were retained. Again, the final calculated diffusivities were not affected. However, it will be seen in Sec. IV that the transit times for completing a single orbit are not long enough for the establishment of the Taylor dispersion limit. Thus, although possible correlation between successive, *single-orbit* transit times does not affect the results, ultimately it is the transit time for completing *multiple* orbits which must be used for measuring the Taylor dispersion coefficient.

B. Particle preparation

The particles used in the experiments were colorless polystyrene beads (manufactured by Maxi-Blast Inc., Southbend, IN; grade PB-2; sieve size 30/45) with radii 0.025 cm$\pm$25 μm and density 1.045 g/cm^3 It was a challenge to color the particles and the only attempt that was successful was to color them using a waterproof marker pen. Marking the particle did not measurably affect the density or radius.

A solution of water and glycerine was prepared which matched the density of the particles. Most of the particles would remain suspended for at least two to three hours, a duration longer than a typical test run. The viscosity of the glycerin/water solution was 1.5 centipoise and so the particle Reynolds numbers, at the rotation rates described below, were of order 10^{-1}.

The principal difficulty using the polystyrene spheres was that they were difficult to wet with water. An effective way of wetting the particles was by first spraying the particles with steam and then immersing them in water, where they remained stored prior to the experiments.

To determine the volume fraction of solids in the suspension, the wetted particles were weighed after blotting out the water adhering to a wet clump of particles, and then the particles were added to the host liquid. The wet particles upset the neutral buoyancy. Hence, glycerin was added dropwise until density matching was restored. From these procedures the water content of the wetted particles was determined. The desired volume fraction was achieved by adding additional density matched host liquid. Typically the cell was filled to a working height of 16 cm and the marked particle introduced at mid-height using a syringe. Transit times were recorded only after the cell was mixed thoroughly.

C. Experiments performed

The alignment of the device was checked by placing a single particle in the cell and rotating the inner cylinder at rotation speeds between 8 and 32 rpm. The variation in successive transit times was within a few tenths of a percent.

Invariably, upon adding the suspension to the Couette cell, bubbles were observed on the walls. The bubbles were easily removed using a piece of tygon tubing. The inner cylinder was first rotated at 4 or 8 rpm for about ten minutes in order to allow any air trapped in the lower bearing to bubble away, thus completely wetting the cell. The cell was then emptied and filled with a known concentration of suspension. The colored tracking particle was added, the suspension mixed, and the inner cylinder was rotated at the desired rpm. Typically, transit times were measured for about 45 minutes.

At a given particle concentration, experiments were conducted at 2, 4, 8, 10 and 12 rpm, as indicated by the servocontroller. The actual rpms were measured directly (these deviated slightly from the nominal values) and used in all the data analysis. The critical rpm for the onset of the Taylor-Couette instability was also measured—above 30 percent concentration a critical rpm was not obtained. Experiments were performed at various particle concentrations, but in this contribution we focus on the results obtained at a volume fraction of $\phi \approx 0.25$. The resulting diffusivities at other concentrations (ranging from 13% to 35% by volume) were all of the same order of magnitude and the experimental error bounds did not allow us to distinguish a clear dependence on volume fraction.

D. General observations

At both the top and bottom of the cell a dense concentration band with height about 5 mm formed. The banding was observed at all concentrations, though was more evident at the lower concentrations, and is presumably due to the small density variations that are inevitable in any batch of particles. The bulk of the cell displayed a uniform concentration. The observation of a small degree of band formation was used to estimate the error in the reported volume fraction. The formation of such dense bands may not be easily detected if the host solution is refractive index matched with the suspended particles.

At concentrations above $\phi \approx 0.25$, it was at times difficult to see the marked particle when it moved close to the inner cylinder. The sighting problem was accentuated at higher rotation rates. While transit time data were being taken, if the operator thought that a missed reading had occurred, the data file was marked (by two rapid clicks on the keyboard) and in the subsequent data analysis, the transit times in the vicinity of that point were discarded.

IV. RESULTS

In the subsequent discussion, in order to illustrate the method, we first present the results based upon transit times for single orbits within the device. The analysis is then repeated using transit times for multiple orbits; it is thus found that one should allow multiple orbits to be completed between transit time measurements in order for Taylor dispersion theory to become applicable.

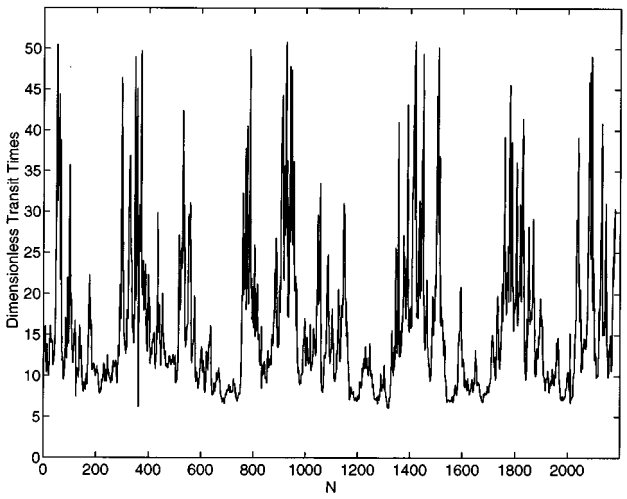

FIG. 2. Measured dimensionless transit times. Experimental data from ten separate experiments at $\phi \approx 0.25$ and five different rpms have been combined, as discussed in the text.

For a given suspension, the Couette experiment was performed many times (between 5 to 15), typically at five different rpms. The particle Reynolds number based on radius, the average shear rate and the viscosity of the suspending medium ranged from 0.05 to 0.3 in our experiments. In each run, several hundred transit times were obtained. Analysis of the data from experiments at different rpms did not reveal a clear trend with varying rpm (i.e., with varying particle Reynolds number); the calculated values of $\hat{D}_{\perp}$ were comparable. Since there seemed to be little hope of distinguishing the dependence on Reynolds number (or rpm) over the narrow range of values studied here, we combined the data sets for the same volume fraction. Thus we report a single value of the shear-induced diffusivity, which represents an average value for particle Reynolds numbers $0.05 < \mathscr{R} < 0.3$.

In order to combine the data sets which were obtained at different rpms, the first step in the analysis was to scale all measured transit times by multiplying each with the value of the angular velocity, Ω, at which it was obtained. As an example, Fig. 2 presents an entire set of dimensionless transit times $\langle \Omega t \rangle$ for ten different experiments at a volume fraction $\phi \approx 0.25$; a total of 2181 transit times were obtained by combining observations at 2, 4, 8, 10 and 12 nominal rpms.

The mean and variance of the collected data are computed easily, providing $\langle \Omega t \rangle$ and $\langle \Omega^2 t^2 \rangle - \langle \Omega t \rangle^2$. From these, the mean angular velocity, Ω^*, and Taylor dispersivity, D^*, can be obtained using equations (15) and (16). Since the Taylor dispersivity (16) involves the product of the cube of the measured Ω^* with the measured variance, it is rather sensitive to errors in either of these quantities. By examining the ''running'' values of the mean and the variance (i.e., by successively including additional data points) we estimate a five to ten percent uncertainty in the final values of the mean and variance of transit times. Hence, the final measured

TABLE I. Experimental results based upon single orbits.

ϕ	N	Ω^*/Ω	D^*/Ω	$\hat{D}_\perp$
0.25	2181	0.40	0.36	1.18

value of D^* and the resulting shear-induced diffusivity $\hat{D}_\perp$ may have as much as forty to fifty percent uncertainty associated with them. This is exacerbated by the fact that the coefficient which relates D^*/Ω to $\hat{D}_\perp$ in (3) is itself a sensitive function of the particle radius a. Therefore, any uncertainty in the particle size, coupled with the fact the suspension is not truly monodisperse, introduces additional errors in the measured values of $\hat{D}_\perp$. Similar uncertainty in $\hat{D}_\perp$ has been reported in the literature (cf. Fig. 5.1 in Phan and Leighton[3]).

The results obtained from combining all the data at $\phi \approx 0.25$ are reported in Table I where the dimensionless shear-induced diffusivity is reported to be $\hat{D}_\perp \approx 1.2$. However, as will be shown below, this result is found not to be accurate since the Taylor dispersion limit is not established during the time it takes the particle to complete a *single* orbit in the device. It should be noted that discarding the data obtained from the second reference line on the Couette device changes the diffusivity to about 1.35. Also, as a test of whether the possible correlation between successive transit times has an effect on the final result, the analysis was repeated after discarding up to ten transit times in between the values that were kept. The diffusivity continued to have a value of $\mathcal{O}(1)$. For completeness, in Table II we also tabulate the experimental results at different rpms before they were combined to produce the results in Table I. No trend in the variation of $\hat{D}_\perp$ with rpm (i.e., Reynolds number) is discernible.

The third column of Table I which reports the measured value of the dimensionless Ω^* can be compared with the theoretically predicted value of 0.45, obtained by evaluating the right hand side of (2). The agreement is reasonable and within the estimated uncertainty.

Once the mean and variance of the transit times have been measured and the long-time transport coefficients Ω^* and D^* calculated, an additional check on the consistency of the data with the proposed theory can be performed by comparing the histogram of measured dimensionless transit times

TABLE II. Breakdown of the $\phi \approx 0.25$ data.

rpm	N	Ω^*/Ω	D^*/Ω	$\hat{D}_\perp$
1.79	82	0.472	0.102	4.24
1.79	106	0.622	0.347	1.24
3.59	90	0.285	0.269	1.60
3.59	94	0.220	0.205	2.10
7.79	344	0.414	0.322	1.34
7.79	259	0.512	0.477	0.90
9.84	314	0.437	0.360	1.20
9.84	250	0.360	0.241	1.79
11.11	425	0.395	0.346	1.25
11.11	223	0.378	0.378	1.14

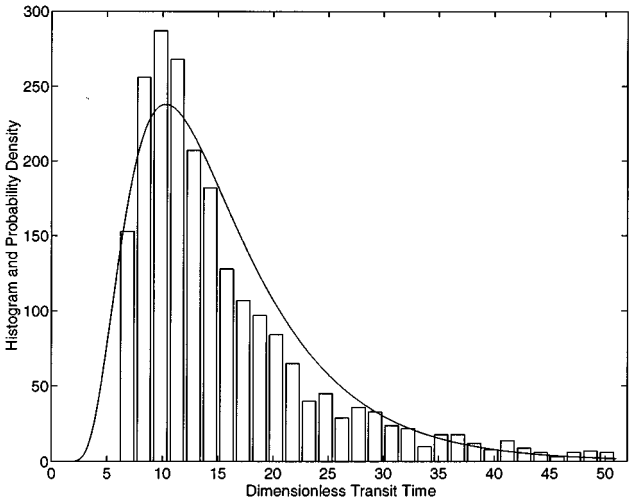

FIG. 3. A histogram of the measured dimensionless transit times. The solid curve is the theoretically predicted probability density function, $f(\tau)$, given by equation (11).

against the predicted probability density function $f(\tau)$. A single parameter q, which is the Peclet number for the mean transport that depends on the measured Ω^* and D^*, fully characterizes the probability density. Figure 3 provides a typical comparison of the two quantities, again for the $\phi \approx 0.25$ data. Of course, the visual appearance of the bar graph representing the histogram is affected by the size and number of ''bins'' which are taken in the interval between zero and the maximum observed transit time. Also, the continuous curve which represents the probability density $f(\tau)$ must be properly scaled by adopting the same nondimensionalization for time as in the data, and by scaling its height so that its integral is consistent with the area under the bar graph. These operations do not introduce any fitting parameters, however. While the visual appearance of the continuous curve and the bar graph is encouraging, a chi-square ''goodness-of-fit'' statistical test indicates that the probability that the two distributions agree is rather small.

Taylor dispersion theory applies only after a long time when the particle has had ample opportunity to sample all radial locations within the Couette device. For a given Couette device, one may need to wait for a particle to complete several orbits in the device, before this long-time limit is achieved. To test our measurements in this way, using the data from just one of the reference lines on the device, we calculated the transit time for completing two, three or more complete orbits and used the successive values of these, in conjunction with the working equations (18) and (19) to calculate the dimensionless shear-induced diffusivity $\hat{D}_\perp$ again. Figure 4 presents $\hat{D}_\perp$ as a function of n, the number of orbits for each transit time. For $n=1$, the value is 1.35 as reported above. As n is allowed to increase, $\hat{D}_\perp$ decreases until, after about 8 or 9 orbits per transit time, it attains a relatively constant value of about 0.13. Note that of the approximately 2200 transit times for single orbits originally measured, about half remain when data from the second reference line are discarded, and by taking the transit times for completing

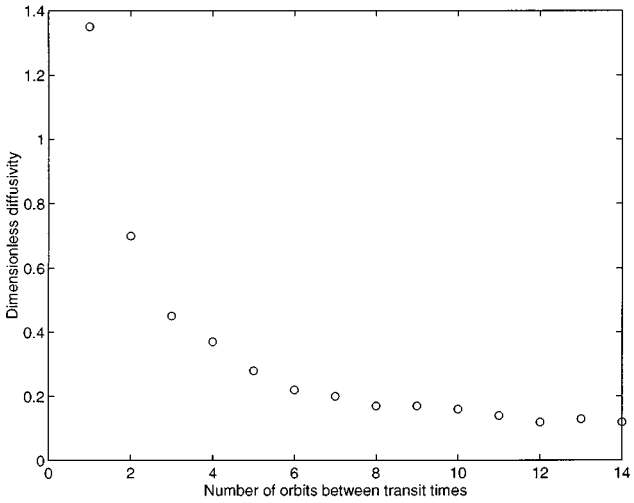

FIG. 4. The dimensionless diffusivity $\hat{D}_\perp$ at $\phi \approx 0.25$ as a function of the number of orbits allowed in between successive transits; its value appears to approach an asymptotic limit of $\mathcal{O}(0.1)$.

14 orbits (the last point in Fig. 4) roughly 75 transit times are available for the calculation.

The dimensionless shear-induced diffusivity measured here at a volume fraction $\phi \approx 0.25$ and a particle Reynolds number of about 10^{-1} has been found to be $\hat{D}_\perp \approx 0.13$ with an uncertainty of about 40%. This result can be compared with the previously reported value of $\hat{D}_\perp \approx 0.04$ measured by Leighton and Acrivos[2] at this volume fraction but at a much lower particle Reynolds number, and with the Stokesian dynamic simulation by Brady[5] who reports a value of $\hat{D}_\perp \approx 0.055$ at $\phi = 0.45$ (the diffusivity is reported to be unchanged at a volume fraction of $\phi = 0.32$ as well[5]). Also, if one uses the best fit parameter $K_c \approx 0.4$ of Phillips *et al.*,[8] obtained at a volume fraction of $\phi \approx 0.5$, the resulting dimensionless diffusivity is $\hat{D}_\perp = K_c \phi \approx 0.2$, at a particle Reynolds number less than approximately 10^{-3}.

V. DISCUSSION

The principal result of this contribution has been to illustrate the possible use of Taylor dispersion theory, as applied to the cylindrical Couette device by Nadim,[6] for the measurement of shear-induced lateral self-diffusivity in concentrated suspensions. The detailed procedure for making such a measurement has been outlined, relying on the newly-derived probability density function for n-orbit transit times, cf. Eq. (17), which yields explicit results relating the mean and variance of such transit times to the mean angular velocity and Taylor dispersion coefficient for azimuthal transport; cf. Eqs. (18) and (19).

The procedure has been applied to a concentrated suspension at a volume fraction of approximately 0.25 for which the shear-induced diffusion coefficient at a particle Reynolds number of $\mathcal{O}(10^{-1})$ has been found to be $D_\perp / (\dot{\gamma} a^2) \approx 0.13$. To obtain this result, it has been found that transit times for completing more that about 8 or 9 orbits in the device are required in order for the particle to be able to sample all radial locations sufficiently for Taylor dispersion theory to become applicable. Although the current uncertainty in the measurement is fairly large, further refinement of the method may permit more accurate measurements of shear-induced diffusivity to be achieved. Our early results suggest that, at larger particle Reynolds numbers, the shear-induced diffusivity is somewhat larger than those obtained at very low Reynolds numbers. In a suspension for which the particle Reynolds number is finite, we might expect even small inertial effects to influence processes such as shear-induced dispersion which rely on many hydrodynamic interactions among the particles. Inertia will affect every ''collision'' and hence after many such collisions small inertial influences may produce a measurable effect. Our measurements are consistent with this idea. We believe that these first-of-their-kind measurements of shear-induced diffusivity using long-time Taylor dispersion data can provide a novel basis for further experimental investigations in this area.

It should be noted that as the volume fraction of particulates tends to zero and the mechanism of lateral migration through collisions or hydrodynamic interactions disappears (thereby causing the shear-induced diffusivity to tend to zero), the Taylor dispersion-based method of analysis loses validity. The reason is that the Taylor dispersion analysis is based on the assumption that there is sufficient time for the tracer to sample all radial locations within the Couette device many times during the experiment. As the lateral diffusivity tends to zero, however, it takes a prohibitively long time, $\mathcal{O}((R_2 - R_1)^2 / D_\perp)$, to reach the Taylor dispersion limit. It is thus impractical to use Taylor dispersion ideas to measure the lateral diffusivity in very dilute suspensions.

Since the particle Reynolds number is not vanishingly small in our experiments, inertial migration effects such as those analyzed by Ho and Leal[9] (who studied the translation of a single particle near a rigid boundary at small but finite $\mathcal{R}$) may also be significant. Such particle-wall effects would tend to concentrate the particles at a radial location nearly half-way between the two cylinders. Our experimental observations did not suggest this to be the case, since the variability in the measured transit times indicated the sampling of all radial locations within the gap.

ACKNOWLEDGMENTS

We thank the Merck Foundation for financial support of the experimental work reported here. Also, HAS gratefully acknowledges the National Science Foundation for support of this work through a PYI Award (CTS-8957043). We thank Professor David Leighton for providing us with a preprint of his recent work, and the referees for their helpful reviews which improved the clarity of the paper.

APPENDIX: DERIVATION OF $f(\tau)$

In this appendix, equation (11) for the probability density of transit times, $f(\tau)$, is derived by means of Laplace transformation. Begin with the dimensionless counterpart of (1):

$$\frac{\partial P}{\partial \tau}+2q\frac{\partial P}{\partial \theta}=\frac{\partial^2 P}{\partial \theta^2}, \tag{A1}$$

where θ has been scaled by 2π, τ is defined by (12), q is given by (13) and $P(\theta,\tau)$ is the renormalized probability density. The initial and boundary conditions are

$$P=\delta(\theta), \quad \text{at } \tau=0, \tag{A2}$$

$$P=0, \quad \text{at } \theta=1, \tag{A3}$$

$$P\to 0, \quad \theta\to-\infty. \tag{A4}$$

Once the solution to the system of equations (A1)–(A4) has been obtained, the first passage time probability density, $f(\tau)$, is determined using the dimensionless counterpart of (10):

$$f(\tau)=-\left.\frac{\partial P}{\partial \theta}\right|_{\theta=1}. \tag{A5}$$

Taking the Laplace transform with respect to τ of (A1) and boundary conditions (A3) and (A4) yields the equations governing the transformed probability density, $\overline{P(\theta,s)}$:

$$\frac{d^2\overline{P}}{d\theta^2}-2q\frac{d\overline{P}}{d\theta}-s\overline{P}=-\delta(\theta), \tag{A6}$$

$$\overline{P}=0, \quad \text{at } \theta=1, \tag{A7}$$

$$\overline{P}\to 0, \ \text{as } \theta\to-\infty. \tag{A8}$$

The solution to the system of equations (A6)–(A8) is

$$\overline{P}=\begin{cases} Ae^{\lambda_2\theta}, & \theta<0, \\ Be^{\lambda_1\theta}+Ce^{\lambda_2\theta}, & \theta>0, \end{cases} \tag{A9}$$

where

$$\lambda_1=q-\sqrt{q^2+s}, \qquad \lambda_2=q+\sqrt{q^2+s}. \tag{A10}$$

The constants of integration are found by using (A7) and satisfying the correct ''jump'' conditions across the origin [obtained by integrating (A6) over an infinitesimal neighborhood of $\theta=0$]. The result is

$$B=\frac{1}{\lambda_2-\lambda_1}, \qquad C=\frac{-e^{-(\lambda_2-\lambda_1)}}{\lambda_2-\lambda_1}, \qquad A=B+C. \tag{A11}$$

It is convenient to determine directly the Laplace transform of the first passage probability, $f(\tau)$, rather than inverting the Laplace transform (A9). In accordance with (A5), we have

$$\overline{f}(s)=-\left.\frac{d\overline{P}}{d\theta}\right|_{\theta=1}=-B\lambda_1 e^{\lambda_1}-C\lambda_2 e^{\lambda_2}=e^{q-\sqrt{q^2+s}}. \tag{A12}$$

The Laplace transform (A12) is inverted easily to yield

$$f(\tau)=\frac{1}{2\sqrt{\pi\tau^3}}\exp\left(q-q^2\tau-\frac{1}{4\tau}\right), \tag{A13}$$

as the equation for the probability density of transit times for a tagged sphere to execute one complete orbit in the Couette device.

[1] E. C. Eckstein, D. G. Bailey, and A. H. Shapiro, ''Self-diffusion of particles in shear flow of a suspension,'' J. Fluid Mech. **79**, 191 (1977).

[2] D. Leighton and A. Acrivos, ''Measurement of the shear-induced self-diffusion in concentrated suspensions of spheres,'' J. Fluid Mech. **177**, 109 (1987).

[3] S. E. Phan and D. T. Leighton, Jr., ''Measurement of the shear-induced tracer diffusivity in concentrated suspensions'' (in preparation).

[4] J. R. Abbott, N. Tetlow, A. L. Graham, S. A. Altobelli, E. Fukushima, L. A. Mondy, and T. S. Stephens, ''Experimental observations of particle migration in concentrated suspensions: Couette flow,'' J. Rheol. **35**, 773 (1991)

[5] J. Brady ''Stokesian dynamics simulation of particulate flow,'' in *Particulate Two-Phase Flow*, edited by M. C. Roco (Butterworth-Heinemann, Boston, 1993), pp. 912–950.

[6] A. Nadim, ''The measurement of shear-induced diffusion in concentrated suspensions with a Couette device,'' Phys. Fluids **31**, 2781 (1988).

[7] H. Brenner and D. A. Edwards, *Macrotransport Processes* (Butterworth-Heinemann, Boston, 1993).

[8] R. J. Phillips, R. C. Armstrong, R. A. Brown, A. L. Graham, and J. R. Abbott, ''A constitutive equation for concentrated suspensions that accounts for shear-induced particle migration,'' Phys. Fluids A **4,** 30 (1992).

[9] B. P. Ho and L. G. Leal, ''Inertial migration of rigid spheres in two-dimensional unidirectional flows,'' J. Fluid Mech. **65,** 365 (1974).